

Photoionisation of Cl⁺ from the $3s^23p^4\ ^3P_{2,1,0}$ and the $3s^23p^4\ ^1D_2, ^1S_0$ states in the energy range 19 - 28 eV

Brendan M. McLaughlin,^{1,2*}

¹*Center for Theoretical Atomic Molecular and Optical Physics (CTAMOP), School of Mathematics and Physics, The David Bates Building, 7 College Park, Queens University Belfast, Belfast BT7 1NN, UK,*

²*Institute for Theoretical Atomic Molecular and Optical Physics (ITAMP), Harvard-Smithsonian Center for Astrophysics, 60 Garden Street, MS-14, Cambridge MA 02138, USA*

Accepted –3 October 2016; Revised 3 October 2016; in original form 15 February 2016

ABSTRACT

Absolute photoionisation cross sections for the Cl⁺ ion in its ground and the metastable states; $3s^23p^4\ ^3P_{2,1,0}$, and $3s^23p^4\ ^1D_2, ^1S_0$, were measured recently at the Advanced Light Source (ALS) at Lawrence Berkeley National Laboratory using the merged beams photon-ion technique at an photon energy resolution of 15 meV in the energy range 19 – 28 eV. These measurements are compared with large-scale Dirac Coulomb *R*-matrix calculations in the same energy range. Photoionisation of this sulphur-like chlorine ion is characterized by multiple Rydberg series of autoionizing resonances superimposed on a direct photoionisation continuum. A wealth of resonance features observed in the experimental spectra are spectroscopically assigned and their resonance parameters tabulated and compared with the recent measurements. Metastable fractions in the parent ion beam are determined from the present study. Theoretical resonance energies and quantum defects of the prominent Rydberg series $3s^23p^3nd$, identified in the spectra as $3p \rightarrow nd$ transitions are compared with the available measurements made on this element. Weaker Rydberg series $3s^23p^3ns$, identified as $3p \rightarrow ns$ transitions and window resonances $3s3p^4(^4P)np$ features, due to $3s \rightarrow np$ transitions are also found in the spectra.

Key words: atomic data – atomic processes – scattering

1 INTRODUCTION

In astrophysics, abundances calculations are based on available atomic data that often are insufficient to make definite identifications of spectroscopic lines (Cardelli et al. 2000). In planetary nebulae, the known emission lines are used to identify a characteristic element resulting from the process of nucleosynthesis in stars (Sharpee et al. 2007; Sterling et al. 2007). The study of photoionisation of sulphur-like ions is of considerable interest because of its abundance in space and the interstellar medium. As previously indicated by Hernández and co-workers (Hernández et al. 2015) there is a wealth of astrophysical applications for this Cl II ion (Cartlidge 2012; Sylwester et al. 2011; Neufeld et al. 2012; Mooney et al. 2012). Sulphur-like chemistry is also of importance in theoretical studies of interstellar shocks (Pineau des Forêts et al. 1986). Photoabsorption and photoionisation processes in the vacuum ultraviolet (VUV) region play an important role in determining solar and stellar opacities (Kohl & Parkinson 1973; Dupree 1978; Lombardi

et al. 1981). The Cl II ion is an important basis for atmospheric and astrophysical models. Determining accurate abundances for sulphur-like chlorine is of great importance in understanding extragalactic H II regions (Garnett 1989) and emission lines of Cl II in the optical spectra of planetary nebulae NGC 6741 and IC 5117 (Keenan et al. 2003). Cl II emission lines have also been seen in the spectra of the Io torus (Küppers & Schneider 2000) and by the far-ultraviolet spectroscopic explorer (FUSE) (Feldman et al. 2001).

In the present study, we use a fully relativistic Dirac Coulomb *R*-matrix approximation (Norrington & Grant 1987; Wijesundera et al. 1991; Norrington 2004; Grant 2007) to interpret and analyze resonance features found in recent high resolution measurements obtained at the ALS (Hernández et al. 2015). In our work we give a detailed interpretation and understanding of the atomic processes involved for single-photon ionization of Cl II forming Cl III. The interaction of a single photon with a Cl II ion comprises contributions from both direct ionization and excitation of autoionizing resonances (Berkowitz 1979). Direct electron ejection processes relevant to the total cross section for single ionization of the Cl⁺ ion in its ground configuration include,

* E-mail:bmclaughlin899@btinternet.com

$$h\nu + \text{Cl}^+(3s^2 3p^4 \ ^3P) \rightarrow \begin{cases} \text{Cl}^{2+}(3s^2 3p^3) + e^- \\ \text{Cl}^{2+}(3s 3p^4) + e^- \end{cases} \quad (1)$$

Indirect ionization of Cl^+ levels within the 3P ground term may proceed via resonance formation

$$h\nu + \text{Cl}^+(3s^2 3p^4 \ ^3P_J) \rightarrow \begin{cases} \text{Cl}^+(3s^2 3p^3 n\ell \ ^3L_{J'}) \\ \text{Cl}^+(3s 3p^4 n\ell' \ ^3L_{J'}) \end{cases} \quad (2)$$

(where, $n\ell = ns$ or nd , and $n\ell' = np$), with subsequent decay by emission of a single electron

$$\text{Cl}^+(^3L_{J'}) \rightarrow \text{Cl}^{2+} + e^-, \quad (3)$$

where L is the total orbital momentum quantum number and J' the total angular momentum quantum number of the intermediate resonant state. Selection rules for electric dipole transitions require that $J' = J$ or $J' = J \pm 1$. Similar types of atomic processes occur for the case where this Cl^+ ion is in the excited metastable states, $3s^2 3p^4 \ ^1D_2$, or 1S_0 .

On the experimental side, measurements of the photoionisation spectrum for this ion have been reported on recently (Hernández et al. 2015). Detailed high-resolution measurements were carried out at an energy resolution of 15 meV full width half maximum (FWHM) using synchrotron radiation at the Advanced Light Source (ALS) in Berkeley, California, for the photon energies in the region 19 - 27.8 eV. Absolute values for the cross section were reported on for the photoionisation of the $^3P_{2,1,0}$ states of the $3s^2 3p^4 \ ^3P$ configuration in this sulphur-like ion, for photon energies in the energy region 23.38 - 27.8 eV, and for the metastable states $3s^2 3p^4 \ ^1D_2$, 1S_0 for photon energies, 19.5 - 27.8 eV. Resonance features observed in the corresponding experimental spectra were analyzed and discussed but no attempt was made to assign and identify the resonance series (Hernández et al. 2015).

On the theoretical side, previous photoionisation cross-section calculations of this ion to the author's knowledge have been rather limited (Opacity Team 1995). We note that accurate transition probabilities (Froese-Fischer 1977; Cowan 1981; Froese-Fischer et al. 1996) and f -values between levels of a system are good indicators of the quality of target wavefunctions used in subsequent cross sections calculations. For electron impact excitation (EIE) of the Cl^{2+} (Cl III) ion, calculations have been reported on using the intermediate coupling approximation by Sossah and Tayal (Sossah & Tayal 2012) within the R -matrix method (Burke & Robb 1975; Burke 2011) although no resonance features were reported. Radiative data for chlorine and its ions has also been reported on by Berrington and Nakazaki (Berrington & Nakazaki 2002) based on R -matrix calculations performed in LS -coupling as no data currently exists in the Opacity Project database (Opacity Team 1995).

The limited high quality data available for the Cl^+ ion is one of the major motivating factors for the present investigations. Identification of the Rydberg resonance series in spectra, in particular the window resonances is another major motivation factor. Understanding the interplay and interaction between the direct and indirect photoionisation processes help us understand and interpret the underlying physics. Furthermore, benchmarking the present large-scale cross section calculations on this ion against available high-resolution experimental results, is essential as it provides

further confidence in the data for use in various laboratory and astrophysical plasma applications.

The layout of this paper is as follows. In Section 2 we outline the theoretical methods employed in our work. Section 3 presents the theoretical results from the DARC photoionisation cross and the resonance analysis. Section 4 presents a comparison between the available experimental measurements (Hernández et al. 2015) and the theoretical cross section results for singly ionized atomic chlorine ground and metastable terms [$\text{Cl}^+(3s^2 3p^4 \ ^3P_{2,1,0})$ and $\text{Cl}^+(3s^2 3p^4 \ ^1D_2, \ ^1S_0)$] in the photon energy range from 19 - 28 eV. Section 5 gives a brief discussion of our results in comparison to the available measurements (Hernández et al. 2015). Finally in Section 6 we give a summary of our findings from our theoretical work.

2 THEORY

2.1 Dirac Coulomb R -matrix

The study of the photoabsorption spectrum of Mid-Z elements and their isoelectronic sequences is very interesting due to the open-shell nature of these complexes and the role played by electron correlation effects. Singly ionized atomic chlorine is one such open-shell ion. In a similar manner to our previous work on atomic sulphur (Barthel et al. 2015), to gauge the quality of our work we carried out large-scale close-coupling calculations and benchmarked the results with the experimental photoionisation cross section measurements (Hernández et al. 2015). The target wavefunctions for our work were obtained using the GRASP code (Dyall et al. 1989; Parpia et al. 2006; Grant 2007), and the subsequent theoretical photoionisation cross sections were obtained with the DARC codes (Ballance 2015). All the target wavefunction orbitals up to $n = 3$ were determined within an EAL calculation using the GRASP code. Target wavefunctions were then generated with all 512 levels arising from the eight configurations: $3s^2 3p^3$, $3s 3p^4$, $3s^2 3p^2 3d$, $3s^2 3p 3d^2$, $3s 3p^3 3d$, $3p^3 3d^2$, $3p^5$, $3s 3p^2 3d^2$, of the residual sulphur singly ionized ion. All these levels were included in the close-coupling expansion. Our photoionisation cross section calculations were performed within the relativistic Dirac-Coulomb R -matrix approximation (Ballance 2015; Grant 2007). An efficient parallel version of the DARC suite of codes has been developed to address the challenge of electron and photon interactions with atomic systems catering for hundreds of levels and thousands of scattering channels.

For comparison with high-resolution measurements made at the ALS, state-of-the-art theoretical methods with highly correlated wavefunctions that include relativistic effects are used. Due to the presence of metastable states in the Cl^+ ion beam experiments additional theoretical calculations were required in order to have a true comparison between theory and experiment. Recent modifications to the Dirac-Atomic R -matrix-Codes (DARC) (Ballance 2015; Ballance & Griffin 2006; McLaughlin & Ballance 2012b,a, 2015; McLaughlin et al. 2015, 2016a) now allow high quality photoionisation cross section calculations to be made (in a timely manner) on heavy complex systems (Fe-peak elements and mid-Z atoms) of prime interest to astrophysics and plasma applications. Cross-section calculations for various trans-Fe element single photoionisation of

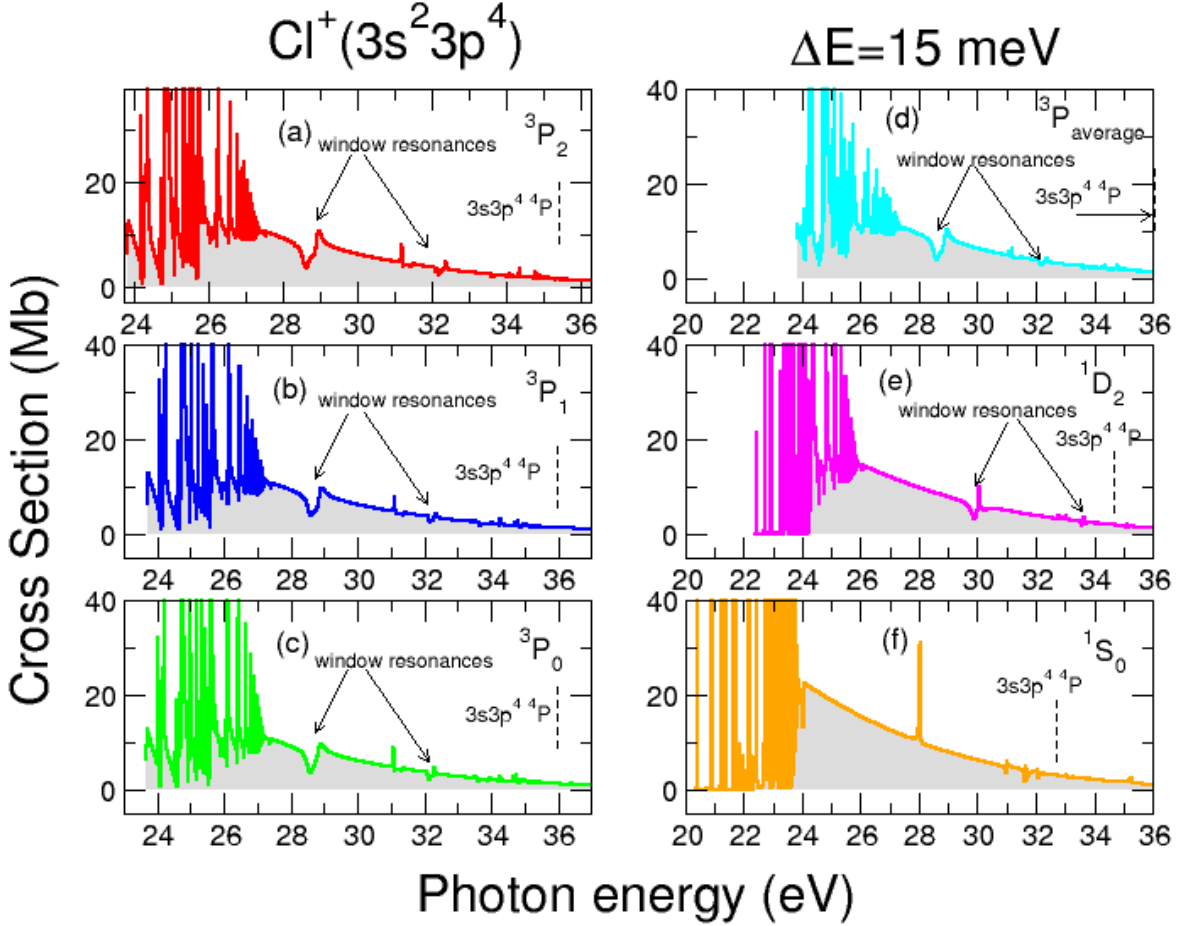


Figure 1. (colour online) Theoretical cross sections from the 512 level DARC calculations for the sulphur-like chlorine ion in the $3s^2 3p^4 \ ^3P_{2,1,0}$, $3s^2 3p^4 \ ^1D_2$, and $3s^2 3p^4 \ ^1S_0$ initial states convoluted with a Gaussian profile of 15 meV. Single photoionisation cross sections of the sulphur-like chlorine ion as a function of energy over the photon energy from thresholds to and energy region just above the $\text{Cl}^{2+}(3s3p^4 \ ^4P)$ threshold, illustrating strong resonance features in the spectra. (a) $3s^2 3p^4 \ ^3P_2$, (b) $3s^2 3p^4 \ ^3P_1$, (c) $3s^2 3p^4 \ ^3P_0$, (d) $3s^2 3p^4 \ ^3P$ level averaged, (e) metastable $3s^2 3p^4 \ ^1D_2$ and (f) metastable $3s^2 3p^4 \ ^1S_0$ cross sections. The corresponding series limits E_∞ of Equation (2) for the window resonances converging to the $3s3p^4 \ ^4P$ threshold is indicated by vertical lines.

Se^+ (McLaughlin & Ballance 2012b), Se^{2+} (Macaluso et al. 2015), Xe^+ (McLaughlin & Ballance 2012a), Kr^+ (Hinojosa et al. 2012), Xe^{7+} (Müller et al. 2014), $2p^{-1}$ inner-shell studies on Si^+ ions (Kennedy et al. 2014), valence-shell studies on neutral sulphur (Barthel et al. 2015), Tungsten and its ions (Ballance & McLaughlin 2015; Müller et al. 2015; McLaughlin et al. 2016b) have been made using these DARC codes. We point out that suitable agreement of DARC photoionisation cross-sections calculations with the above high resolution measurements made at leading synchrotron light sources such as ALS, ASTRID, SOLEIL and PETRA III has been obtained.

2.2 Photoionisation

To benchmark theory with the recent ALS measurements of photoionisation cross-sections (Hernández et al. 2015),

calculations on this sulphur-like ion were performed on the ground and the excited metastable levels associated with the $3s^2 3p^4$ configuration. Hibbert and co-workers have shown that two-electron promotions are important to include to get accurate energies, f -values and Einstein coefficients (Ohja & Hibbert 1987; Keenan et al. 1993) which are included in the present study. In our photoionisation cross-section calculations for this element, all 512 levels arising from the eight configurations: $3s^2 3p^3$, $3s3p^4$, $3s^2 3p^2 3d$, $3s^2 3p3d^2$, $3s3p^3 3d$, $3p^3 3d^2$, $3p^5$, $3s3p^2 3d^2$ of the residual chlorine doubly ionized ion were included in the close-coupling expansion. In our calculations for the ground and metastable levels, the outer region electron-ion collision problem was solved with an extremely fine energy mesh of $0.272 \mu\text{eV}$ to fully resolve the extremely narrow resonance features found in the appropriate photoionisation cross sections.

Photoionisation cross section calculations with this 512-

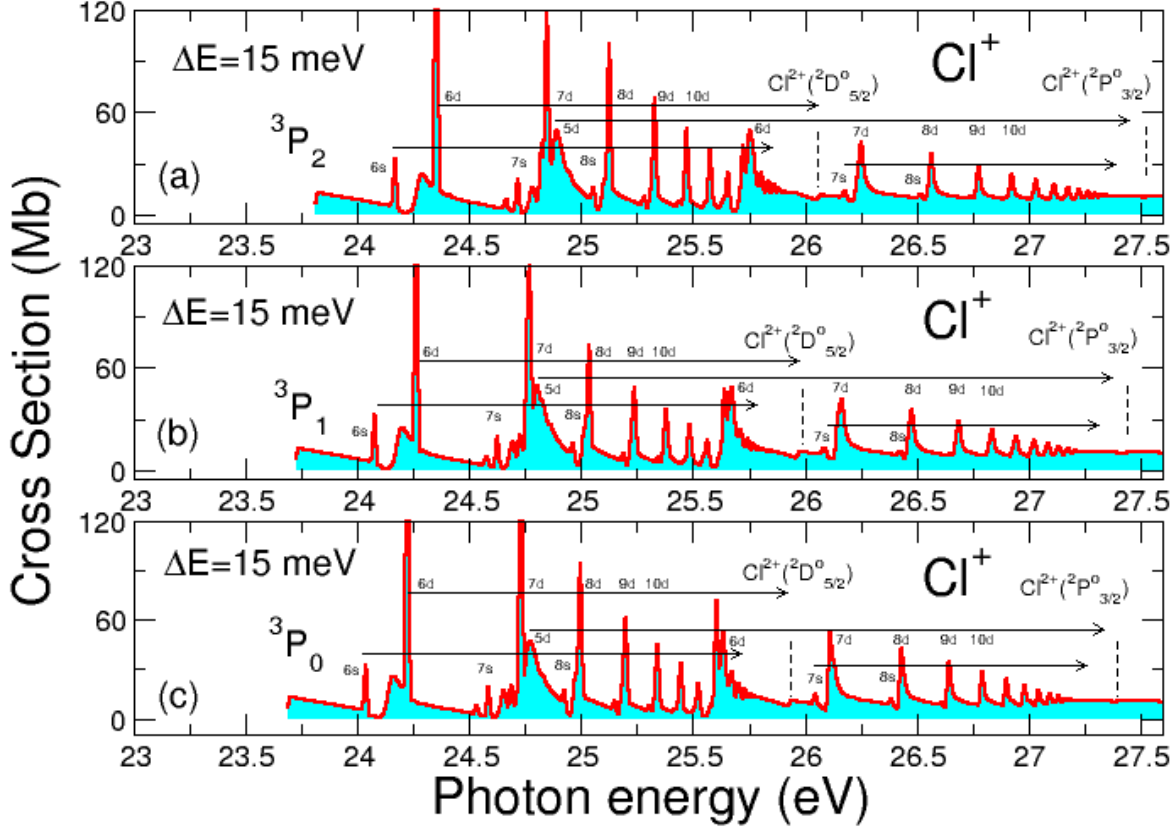


Figure 2. (colour online) Single photoionisation of the sulphur-like chlorine ion as a function of the photon energy from the $3s^23p^4\ ^3P_{2,1,0}$ states from threshold to 27.6 eV. (a) $3s^23p^4\ ^3P_2$, (b) $3s^23p^4\ ^3P_1$, and (c) $3s^23p^4\ ^3P_0$. Strong $3s^23p^3(^2D_{5/2}^o)nd$ Rydberg series are present as are the much weaker $3s^23p^3(^2D_{5/2}^o)ns$ series converging to the $\text{Cl}^+(^2D_{5/2}^o)$ threshold. Similar strong $3s^23p^3(^2P_{3/2}^o)nd$ Rydberg series are present as are the much weaker $3s^23p^3(^2P_{3/2}^o)ns$ series converging to the $\text{Cl}^+(^2P_{3/2}^o)$ threshold. Theoretical cross section calculations were carried out with the DARC codes, and convoluted with a Gaussian having a profile of 15 meV. The assigned Rydberg series are indicated as vertical lines grouped by horizontal lines. The corresponding series limits E_∞ of Equation (2) for each series are indicated by a vertical lines at the end of the line groups. Several of the nd interloping resonances are seen to disrupt the regular Rydberg resonance pattern of the spectra. Resonance energies and quantum defects for the various series are tabulated in Tables 1 and 2 and compared with the available experimental values.

level model were performed for the 3P_2 ground and the metastable $^3P_{1,0}$, 1D_2 and 1S_0 states of this ion, over the photon energy range similar to experimental studies. All the cross section calculations were carried out within the Dirac-Coulomb R -matrix approximation (Ballance 2015; Ballance & Griffin 2006; McLaughlin & Ballance 2012b,a, 2015; McLaughlin et al. 2015).

The $^3P_{2,1,0}$ levels require the bound-free dipole matrices, $J^\pi = 2^e, 1^e, 0^e \rightarrow J'^\pi = 0^o, 1^o, 2^o, 3^o$ and for the excited 1D_2 and 1S_0 metastable states, the bound-free dipole matrices, $J^\pi = 0^e, 2^e \rightarrow J'^\pi = 1^o, 2^o, 3^o$. It was necessary to carry out these additional photoionisation cross-section calculations to span the entire photon energy range of the experimental measurements, where various metastable states

are present in the beam in order to have a true comparison between theory and experiment. The jj -coupled Hamiltonian diagonal matrices were adjusted so that the theoretical term energies matched the recommended experimental values of the NIST tabulations (Ralchenko et al. 2014). We note that this energy adjustment ensures better positioning of resonances relative to all thresholds included in the present calculations.

2.3 Resonances

The energy levels available from the NIST tabulations (Ralchenko et al. 2014) were used as a helpful guide for the present assignments. The resonance series identification can

Table 1. Principal quantum numbers n , resonance energies (eV), and quantum defects μ of the $\text{Cl}^+(3s^23p^3[{}^2D_{5/2}^o])ns, nd$ Rydberg series seen in the $\text{Cl}^+(3s^23p^4\ {}^3P_{2,1,0})$ photoionisation spectra, converging to the $\text{Cl}^+(3s^23p^3[{}^2D_{5/2}^o])$ threshold. The experimental resonance energies (Hernández et al. 2015) are calibrated to ± 13 meV. The theoretical results are obtained from the 512-level DARC calculations performed within the Dirac Coulomb R -matrix approximation. The experimental entries in parenthesis are uncertain.

Cl^+ (Initial State)		E_n (eV) Expt ^a	E_n (eV) Theory ^b	μ Expt ^a	μ Theory ^b	E_n (eV) Expt ^a	E_n (eV) Theory ^b	μ Expt ^a	μ Theory ^b
$3s^23p^4\ {}^3P_2$	n		$3s^23p^3({}^2D_{5/2}^o)nd$			$3s^23p^3({}^2D_{5/2}^o)ns$			
	6	24.348	24.353	0.38	0.35		24.166		0.64
	7	24.829	24.846	0.35	0.30		24.710		0.64
	8	25.128	25.130	0.36	0.35		25.056		0.64
	9	25.335	25.334	0.34	0.34		25.283		0.63
	10	25.479	25.476	0.32	0.35				
	11	25.583	25.584	0.32	0.30				
	...								
	∞	26.060 ^c	26.060 ^c			26.060 ^c	26.060 ^c		
	n		$3s^23p^3({}^2D_{5/2}^o)nd$			$3s^23p^3({}^2D_{5/2}^o)ns$			
$3s^23p^4\ {}^3P_1$	6	24.259	24.264	0.37	0.36		24.075		0.65
	7	24.750	24.762	0.33	0.30		24.630		0.64
	8	25.036	25.039	0.38	0.37				
	9	25.238	25.237	0.40	0.40				
	10	25.384	25.385	0.42	0.40				
	11	(25.492)	25.493	(0.37)	0.36				
	...								
	∞	25.974 ^c	25.974 ^c			25.974 ^c	25.974 ^c		
	n		$3s^23p^3({}^2D_{5/2}^o)nd$			$3s^23p^3({}^2D_{5/2}^o)ns$			
	6	24.219	24.223	0.37	0.36		24.041		0.64
$3s^23p^4\ {}^3P_0$	7		24.733		0.27		24.591		0.64
	8	(25.000)	24.999	(0.38)	0.38		24.926		0.64
	9		25.198		0.40				
	10		25.345		0.40				
	...								
	∞	25.936 ^c	25.936 ^c			25.936 ^c	25.936 ^c		

^aALS experimental results (Hernández et al. 2015).

^bPresent R -matrix DARC calculations.

^cRydberg series limits E_∞ for Cl^+ are from the NIST tabulations (Ralchenko et al. 2014).

be made from Rydberg's formula (Rydberg 1890, 1893, 1894; Eisberg & Resnik 1985) :

$$\epsilon_n = \epsilon_\infty - \frac{\mathcal{Z}^2}{\nu^2} \quad (4)$$

where in Rydbergs ϵ_n is the transition energy, ϵ_∞ is the ionization potential of the excited electron to the corresponding final state ($n = \infty$), i.e. the resonance series limit and n being the principal quantum number. The relationship between the principal quantum number n , the effective quantum number ν and the quantum defect μ for an ion of effective charge \mathcal{Z} is given by $\nu = n - \mu$ (Shore 1967; Seaton 1983). Converting all quantities to eV we can represent the Rydberg series as;

$$E_n = E_\infty - \frac{\mathcal{Z}^2 R}{(n - \mu)^2} \quad (5)$$

Here, E_n is the resonance energy, E_∞ the resonance series limit, \mathcal{Z} is the charge of the core (in this case $\mathcal{Z} = 2$), μ is the quantum defect, being zero for a pure hydrogenic state.

For a hydrogenic system this can be written as,

$$E_n^H = E_\infty - \frac{\mathcal{Z}^2 R}{n^2} \quad (6)$$

where the Rydberg constant R is 13.605698 eV.

The multi-channel R -matrix eigenphase derivative (QB) technique, which is applicable to atomic and molecular complexes, as developed by Berrington and co-workers (Quigley & Berrington 1996; Quigley et al. 1998; Ballance et al. 1999) was used to locate and determine the resonance positions. The resonance width Γ may also be determined from the inverse of the energy derivative of the eigenphase sum at the resonance energy E_r via

$$\Gamma = 2 \left[\frac{d\delta}{dE} \right]_{E=E_r}^{-1} = 2 [\delta']_{E=E_r}^{-1}. \quad (7)$$

Finally, in order to compare with experimental, the theoretical cross-section calculations were convoluted with a Gaussian having a profile of width similar to the ALS experiment resolution (15 meV FWHM). Due to the presence of

Table 2. Principal quantum numbers n , resonance energies (eV), and quantum defects μ of the $\text{Cl}^+(3s^23p^3[{}^2P_{3/2}^o])ns, nd$ Rydberg series seen in the $\text{Cl}^+(3s^23p^4\ {}^3P_{2,1,0})$ photoionisation spectra, converging to the $\text{Cl}^+(3s^23p^3[{}^2P_{3/2}^o])$ threshold. The experimental resonance energies (Hernández et al. 2015) are calibrated to ± 13 meV. The theoretical results are obtained from the 512-level DARC calculations performed within the Dirac Coulomb R -matrix approximation. The experimental entries in parenthesis are uncertain.

Cl^+ (Initial State)		$E_n(\text{eV})$ Expt ^a	$E_n(\text{eV})$ Theory ^b	μ Expt ^a	μ Theory ^b	$E_n(\text{eV})$ Expt ^a	$E_n(\text{eV})$ Theory ^b	μ Expt ^a	μ Theory ^b
$3s^23p^4\ {}^3P_2$	n		$3s^23p^3({}^2P_{3/2}^o)nd$				$3s^23p^3({}^2P_{3/2}^o)ns$		
	5	(24.869)	24.880	(0.47)	0.46				
	6	(25.745)	25.754	(0.47)	0.45				
	7	26.246	26.253	0.47	0.45		26.180		0.63
	8	26.564	26.576	0.46	0.46		26.519		0.63
	9	26.778	26.780	0.45	0.44				
	10	26.928	26.927	0.43	0.44				
	11	27.031	27.035	0.47	0.43				
	12	(27.114)	27.115	(0.45)	0.44				
	13	27.175	27.178	0.48	0.42				
	...								
	∞	27.522 ^c	27.522 ^c			27.522 ^c	27.522 ^c		
$3s^23p^4\ {}^3P_1$	n		$3s^23p^3({}^2P_{3/2}^o)nd$				$3s^23p^3({}^2P_{3/2}^o)ns$		
	5	(24.783)	24.804	(0.47)	0.45				
	6	(25.660)	25.668	(0.46)	0.45				
	7	26.157	26.162	0.47	0.46		26.088		0.64
	8	26.475	26.480	0.47	0.45		26.429		0.64
	9	26.687	26.695	0.46	0.43				
	10	26.833	26.842	0.49	0.42				
	...								
	∞	27.435 ^c	27.435 ^c			27.435 ^c	27.435 ^c		
$3s^23p^4\ {}^3P_0$	n		$3s^23p^3({}^2P_{3/2}^o)nd$				$3s^23p^3({}^2P_{3/2}^o)ns$		
	5	(24.714)	24.767	(0.50)	0.45				
	6		25.635		0.44		26.048		0.65
	7	26.108	26.117	0.51	0.48		26.383		0.68
	8	26.430	26.434	0.50	0.49				
	9	26.648	26.650	0.49	0.47				
	10		26.797		0.48				
	...								
	∞	27.398 ^c	27.398 ^c			27.398 ^c	27.398 ^c		

^aALS experimental results (Hernández et al. 2015).

^bPresent R -matrix DARC calculations.

^cRydberg series limits E_∞ for Cl^+ are from the NIST tabulations (Ralchenko et al. 2014).

metastable states in the Cl^+ ion beam experiments, a suitable admixture of the theoretical initial state populations was required. Details are outlined in the following sections.

3 RESULTS

3.1 Cross Sections

The electronic ground-state term of singly ionized atomic chlorine in LS coupling is $3s^23p^4\ {}^3P$ and by spin-orbit effects splits into the three fine-structure states namely, $3s^23p^4\ {}^3P_{2,1,0}$. The difference in energy between the ground state $3s^23p^4\ {}^3P_2$, the metastable $3s^23p^4\ {}^3P_1$, and $3s^23p^4\ {}^3P_0$ states is 86.3 and 123.5 meV (Ralchenko et al. 2014), respectively. Since additional metastable states, $3s^23p^4\ {}^1S_0$, 1D_2

are present in the parent ion beam of the ALS experiments, cross-section calculations for these states were required to span the energy region investigated. In order to simulate the experimental conditions the theoretical cross section are convoluted with a Gaussian having a 15 meV full width half maximum (FWHM) profile and an appropriate fraction of all these excited states are required to compare theory directly with experiment.

Fig. 1 shows an overview of our results for all five initial states of this sulphur-like ion convoluted with a Gaussian of 15 meV FWHM from their respective thresholds up to a photon energy just above the $3s3p^4\ {}^4P$ state of the doubly ionized chlorine ion. As seen from Fig. 1 strong resonances are found in the spectra below about 27 eV. Above the $\text{Cl}^{2+}({}^2P_{3/2}^o)$ threshold a prominent series of window

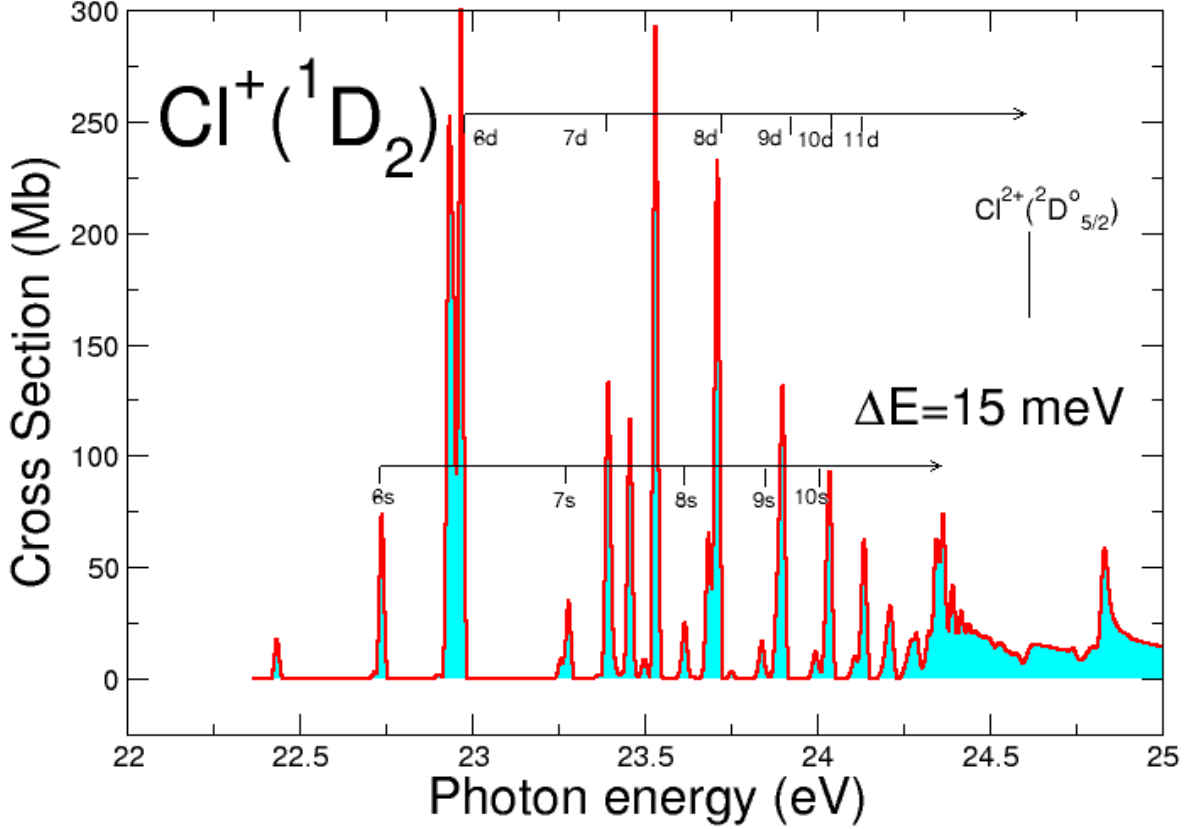


Figure 3. (colour online) Single photoionisation of the sulphur-like chlorine ion as a function of the photon energy in the $3s^23p^4\ ^1D_2$ metastable state from threshold to 25 eV. Theoretical cross section were carried out with the DARC codes, and convoluted with a Gaussian having a profile of 15 meV. The assigned Rydberg series are indicated as vertical lines grouped by horizontal lines. The corresponding series limits E_∞ of Equation (2) for each series are indicated by a vertical line at the end of the line groups. The strong $3s^23p^3(^2D_{5/2}^o)nd$ Rydberg series are present as are the much weaker $3s^23p^3(^2D_{5/2}^o)ns$ series converging to the $\text{Cl}^+(^2D_{5/2}^o)$ threshold. Several of the nd interloping resonances are seen to disrupt the regular Rydberg resonance pattern of the spectra. The first few values of n for each series is displayed close to its corresponding vertical line in each group. Resonance energies and quantum defects for the various series are tabulated in Table 3 and compared with the available experimental values.

resonances $3s3p^4(^4P)np$ converging to the $\text{Cl}^{2+}(3s3p^4\ ^4P)$ threshold is clearly visible in the spectra. The origin of such window resonances has already been discussed in our recent work on atomic sulphur (Barthel et al. 2015). Suffice it is to say that in atomic sulphur, the $3s3p^4\ ^4P$ and $3s3p^4\ ^2P$ ionization states (occurring from a $3s$ vacancy state) are located at 19.056 eV and 22.105 eV, respectively, and two prominent Rydberg series of window resonances were found. We note that similar types of structures were observed by Angel and Samson (Angel & Samson 1988) in atomic oxygen, in atomic selenium, by Gibson and co-workers (Gibson et al. 1986), and atomic tellurium, by Berkowitz and co-workers (Berkowitz et al. 1981). A detailed discussion of the various resonance features found in the respective theoretical spectra for this sulphur-like chlorine ion is presented below and

comparisons made with the high resolution measurements recently made at the ALS (Hernández et al. 2015).

3.2 Photoionisation of the $\text{Cl}^+(3s^23p^4\ ^3P_{2,1,0})$ states

Photoionisation of singly ionized atomic chlorine from the initial $3s^23p^4\ ^3P_{2,1,0}$ fine-structure levels was investigated using large-scale R -matrix calculations within the Dirac Coulomb approximation (DARC). The electronic configuration of the doubly ionized chlorine ion (Cl^{2+}) in the $3s^23p^3$ configuration forms the states $^4S_{3/2}^o$, $^2D_{3/2,5/2}^o$, and $^2P_{1/2,3/2}^o$. As illustrated in Fig. 2, the strongest Rydberg resonances series in the respective $3s^23p^4\ ^3P_{2,1,0}$ spectra converging to the $\text{Cl}^{2+}(^2D_{5/2}^o)$ and $\text{Cl}^{2+}(^2P_{3/2}^o)$

Table 3. Principal quantum numbers n , resonance energies (eV), and quantum defects μ of the $\text{Cl}^+(3s^23p^3[{}^2P_{1/2}^o])ns, nd$ and $\text{Cl}^+(3s^23p^3[{}^2D_{5/2}^o])ns, nd$ Rydberg series seen in the $\text{Cl}^+(3s^23p^4\ {}^1D_2$ and 1S_0) photoionisation spectra, converging to the $\text{Cl}^+(3s^23p^3[{}^2P_{1/2}^o])$ and $\text{Cl}^+(3s^23p^3[{}^2P_{1/2}^o])$ thresholds. The theoretical results are obtained from the 512-level DARC calculations performed within the Dirac Coulomb R -matrix approximation. The experimental values for the resonance energies (Hernández et al. 2015) are from the recent ALS measurements calibrated to ± 13 meV uncertainty. The experimental entries in parenthesis are uncertain.

Cl^+ (Initial State)	$E_n(\text{eV})$ Expt ^a	$E_n(\text{eV})$ Theory ^b	μ Expt ^a	μ Theory ^b	$E_n(\text{eV})$ Expt ^a	$E_n(\text{eV})$ Theory ^b	μ Expt ^a	μ Theory ^b
$3s^23p^4\ {}^1S_0$	n	$3s^23p^3({}^2P_{1/2}^o)nd$			$3s^23p^3({}^2P_{1/2}^o)ns$			
	4	20.426	20.420	0.13	0.13			
	5	21.742	21.734	0.15	0.16	21.235		0.61
	6	22.463	22.459	0.15	0.16	22.191		0.60
	7	22.900	22.890	0.13	0.16	22.724		0.60
	8	23.178	23.170	0.12	0.15	23.061		0.60
	9		23.361		0.14	23.282		0.60
	...							
	∞	24.054 ^c	24.054 ^c		24.054 ^c	24.054 ^c		
	n	$3s^23p^3({}^2D_{5/2}^o)nd$			$3s^23p^3({}^2D_{5/2}^o)ns$			
$3s^23p^4\ {}^1D_2$	6	22.979	22.969	0.27	0.25	22.741		0.61
	7		23.392		0.32	23.278		0.62
	8	23.718	23.719	0.21	0.21	23.616		0.62
	9	23.907	23.907	0.23	0.23	23.841		0.62
	10	24.040	24.039	0.27	0.28	23.995		0.63
	11	(24.152)	24.138	(0.27)	0.32			
	...							
	∞	24.615 ^c	24.615 ^c		24.615 ^c	24.615 ^c		

^aALS experimental results (Hernández et al. 2015).

^bPresent R -matrix DARC calculations.

^cRydberg series limits E_∞ for Cl^+ are from the NIST tabulations (Ralchenko et al. 2014).

thresholds are the $3s^23p^3({}^2D_{5/2}^o)nd$ and $3s^23p^3({}^2P_{3/2}^o)nd$ type series. Weaker Rydberg series $3s^23p^3({}^2D_{5/2}^o)ns$ and $3s^23p^3({}^2P_{3/2}^o)ns$ are also found in the respective theoretical spectra. Only the energies and quantum defects of the prominent $3s^23p^3nd$ series were tabulated in the ALS experimental work (Hernández et al. 2015) but were not spectroscopically assigned. A detailed discussion of such Rydberg series has already been given in our recent study on atomic sulphur (Barthel et al. 2015) and will not be expanded upon here. Suffice it is to say that the dominant series is the $3s^23p^3nd$ with the weaker series being the $3s^23p^3ns$. The energies and quantum defects are tabulated in Table 1 for both types of series converging to the $\text{Cl}^{2+}({}^2D_{5/2}^o)$ threshold and in Table 2 converging to $\text{Cl}^{2+}({}^2P_{3/2}^o)$ threshold for all the respective $3s^23p^4\ {}^3P_{2,1,0}$ initial states. From Tables 1 and 2 excellent agreement of our theoretical values with the available high resolution results from the ALS for the prominent $3s^23p^3nd$ Rydberg series is seen. The majority of the theoretical energies for the respective $3s^23p^3nd$ Rydberg resonance series are within the ± 13 meV experimental uncertainty. As illustrated in Fig. 2, the $5d$ and $6d$ members of the $3s^23p^3({}^2P_{3/2}^o)nd$ series are interloping resonances, lying below the $\text{Cl}^{2+}({}^2D_{5/2}^o)$ threshold and perturbing the spectrum of the $3s^23p^3({}^2D_{5/2}^o)nd$ Rydberg resonance series. Finally, we have also tabulated several members of the weaker

$3s^23p^3ns$ Rydberg series found in the theoretical spectrum in Tables 1 and 2 for completeness.

3.3 Photoionisation of the metastable $\text{Cl}^+(3s^23p^4\ {}^1D_2$, and ${}^1S_0)$ states

Photoionisation cross section calculations of the singly ionized atomic chlorine ion from the initial $3s^23p^4\ {}^1D_2$ and 1S_0 metastable states were also investigated using the same large-scale R -matrix model within the Dirac Coulomb approximation (DARC), as these states were present in the parent ion beam of the recent ALS measurements (Hernández et al. 2015). Fig. 3 shows the results for the $3s^23p^4\ {}^1D_2$ initial state and Fig. 4 the corresponding $3s^23p^4\ {}^1S_0$ case. Cross sections calculations are shown for photon energies from their respective thresholds to a photon energy of 25 eV and convoluted with a Gaussian having a profile width of 15 meV. Here again strong $3s^23p^3({}^2D_{5/2}^o)nd$ and $3s^23p^3({}^2P_{1/2}^o)nd$ Rydberg resonance series and the much weaker $3s^23p^3({}^2D_{5/2}^o)ns$ and $3s^23p^3({}^2P_{1/2}^o)ns$ series are found in the respective spectra.

The energies and quantum defects of all the Rydberg series are tabulated in Table 3 for both series converging to the $\text{Cl}^{2+}({}^2P_{1/2}^o)$ and $\text{Cl}^{2+}({}^2D_{5/2}^o)$ thresholds for each of the respective $3s^23p^4\ {}^1D_2$ and 1S_0 initial states. The available ALS experimental results are included in Table 3 for comparison purposes. From Table 3, for the $3s^23p^3nd$ Rydberg

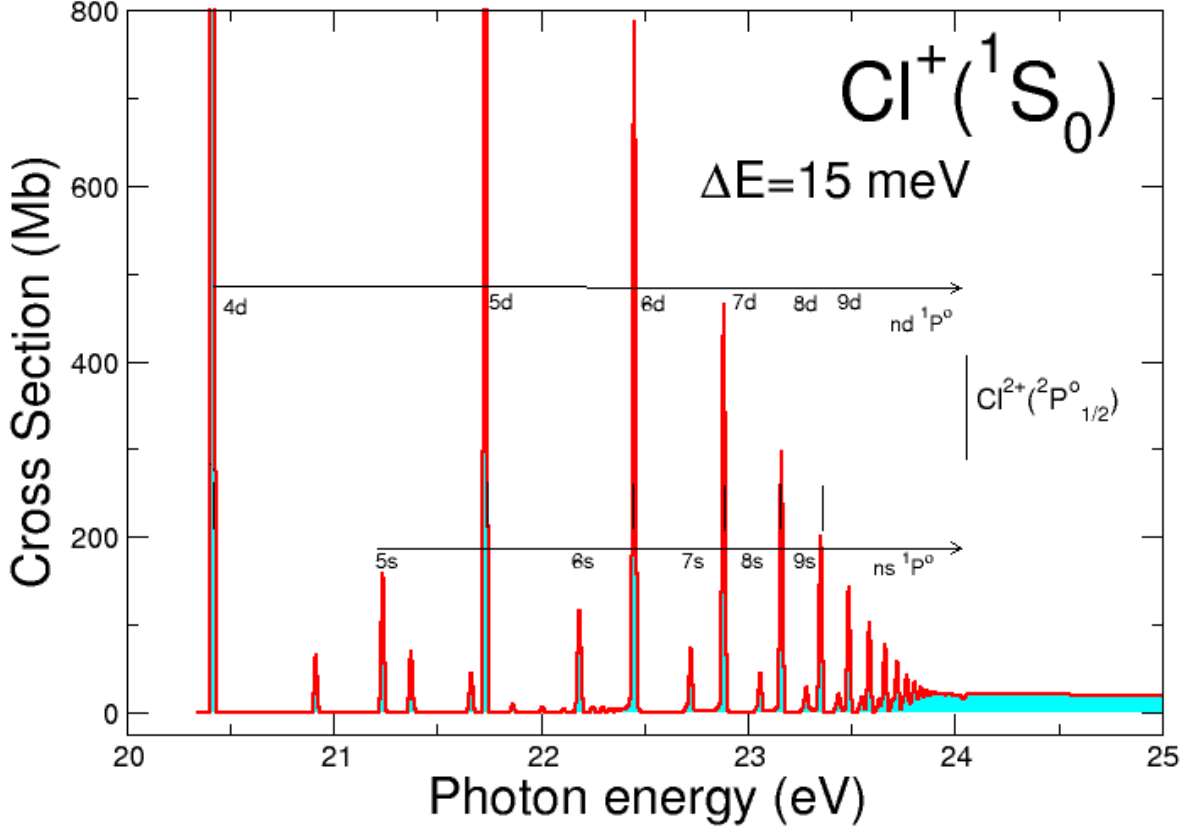


Figure 4. (colour online) Single photoionisation of the sulphur-like chlorine ion as a function of the photon energy in the $3s^23p^4\ ^1S_0$ metastable state from threshold to 25 eV. Theoretical cross section calculations were carried out with the DARC codes, and convoluted with a Gaussian having a profile of 15 meV. The assigned Rydberg series are indicated as vertical lines grouped by horizontal or inclined lines. The corresponding series limits E_∞ of Equation (2) for each series are indicated by a vertical lines at the end of the line groups. The strong $3s^23p^3(^2P_{1/2}^\circ)nd$ Rydberg series are present as are the much weaker $3s^23p^3(^2P_{1/2}^\circ)ns$ series converging to the $\text{Cl}^+(^2P_{1/2}^\circ)$ threshold. Resonance energies and quantum defects for the various series are tabulated in Table 3 and compared with the available experimental values

series, we see excellent agreement between the theoretical values and the available ALS experimental measurements. It is seen that the theoretical values for the resonance energies are within the ± 13 meV energy uncertainty of experiment. This provides additional confidence in our cross sections results which are suitable for many applications in astronomy and astrophysics and for laboratory plasma physics applications.

4 THEORY AND EXPERIMENT COMPARISON

To simulate experiment the theoretical photoionisation cross sections for each initial state was convoluted at the experimental resolution of 15 meV and a suitable admixture of the initial states present in the beam carried out.

Fig. 5 illustrates the comparison of our DARC calculations on the ground and metastable states of this sulphur-like chlorine ion with the recent measurements from the ALS (Hernández et al. 2015). In Fig. 5 we have convoluted the theoretical cross sections with a Gaussian having a profile width of 15 meV FWHM in order to compare with the experimental measurements. To achieve the best match of the high resolution measurements made at the ALS (Hernández et al. 2015) with the DARC results we find that a non-statistical weighting of the theoretical data for initial states of this sulphur-like chlorine ion was as follows; 1% of the $3s^23p^4\ ^1S_0$ state, 27% of the $3s^23p^4\ ^1D_2$ state, the other 72% distributed among the $3s^23p^4\ ^3P_{2,1,0}$ fine-structure levels, namely; 40% 3P_2 , 24% 3P_1 and 8% 3P_0 . This weighting of the initial states of the theoretical photoionisation cross

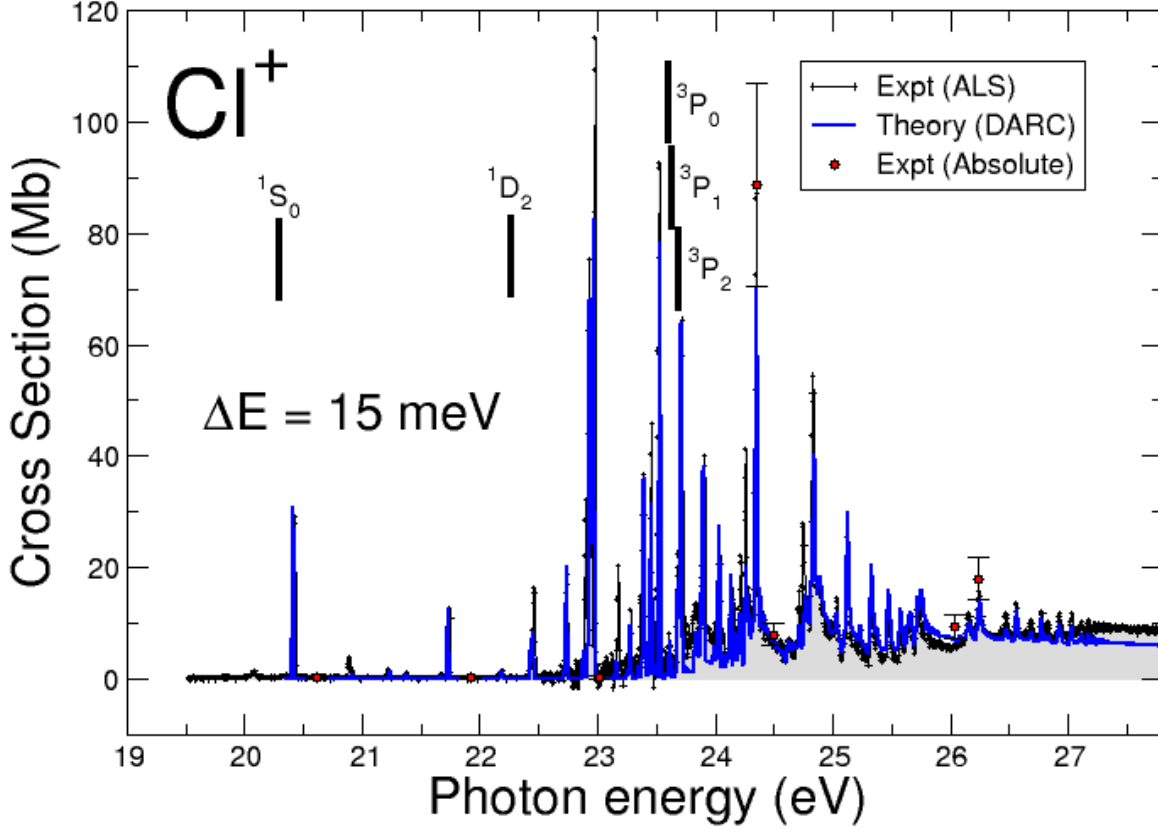


Figure 5. (colour online) Single photoionisation of the sulphur-like chlorine ion as a function of the photon energy in the energy region 19 - 27.5 eV. The experimental results shown are from the recent high resolution measurements made at the ALS at a resolution of 15 meV FWHM (Hernández et al. 2015). The theoretical cross section calculations are from large-scale DARC calculations convoluted with a Gaussian having a profile of 15 meV FWHM. An appropriate weighting has been used for the ground and metastable states of this sulphur-like chlorine ion to best match the high resolution ALS experimental measurements (see text for details).

sections appears to accurately reproduce the spectra in the high resolution ALS measurements.

An additional check on the theoretical data is the comparison of the integrated continuum oscillator strength f with experiment. The integrated continuum oscillator strength f of the experimental spectra was calculated over the energy grid $[E_1, E_2]$, where E_1 is the minimum experimental energy and E_2 is the maximum experimental energy measured, (respectively 19.5 eV and 28 eV), using (Shore 1967; Fano & Cooper 1968; Berkowitz 1979),

$$f = 9.1075 \times 10^{-3} \int_{E_1}^{E_2} \sigma(h\nu) d h\nu \quad (8)$$

and yielded a value of 0.473 ± 0.095 from the ALS measurements. A similar procedure for the theoretical R -matrix cross section (from appropriated weighted initial states) gave a value of 0.405, in good agreement with experiment. This allows one to quantify an error estimate which we conservatively give as 15% for the theoretical cross sections.

5 CONCLUSIONS

Large-scale Dirac Coulomb R -matrix (DARC) photoionisation cross section calculations have been carried for the singly ionised chlorine ion for the $3s^23p^4\ ^3P_{2,1,0}$, $3s^23p^4\ ^1D_2$ and $3s^23p^4\ ^1S_0$ initial states in the energy range 19 - 28 eV. For a physical understanding of the atomic processes taking place, we analyze the autoionizing resonance features found in the spectra. Strong Rydberg series of the type $3s^23p^3nd$ along with much weaker series of the form $3s^23p^3ns$ are found in the respective photoionisation spectra. All these resonance series are analyzed, compared and contrasted with recently reported high resolution measurements made at the ALS and spectroscopically assigned. Excellent agreement of the present theoretical photoionisation cross sections with recent ALS measurements (Hernández et al. 2015) is found. This essential benchmarking of the theoretical work against high-resolution measurements provides confidence in the data for applications.

6 SUMMARY

The photoionisation cross sections for the singly ionized atomic chlorine ion in the states $3s^23p^4\ ^3P_{2,1,0}$, and $3s^23p^4\ ^1D_2$ and $3s^23p^4\ ^1S_0$ were calculated using the Dirac Coulomb *R*-matrix (DARC) method in the experimentally studied energy region of 19 - 28 eV. Numerous autoionization resonances features are found in the photoionisation spectra and their resonance energies and quantum defects tabulated and compared with recent ALS measurements (Hernández et al. 2015). Various interloping resonances are found in the photoionisation spectra from the different initial states of this sulphur-like species. The interloping resonances are seen to disrupt the regular Rydberg series pattern in the spectra. Overall the resonance features found in the theoretical spectra obtained using the DARC codes in the valence photon energy region show excellent agreement with previous ALS measurements (Hernández et al. 2015) and are within the ± 13 meV energy uncertainty of experiment.

The high resolution experimental measurements made at the ALS synchrotron radiation facility (over a limited energy range) have been used to benchmark the theoretical calculations, and as such our theoretical work would be suitable to be incorporated into astrophysical modelling codes like CLOUDY (Ferland et al. 1998; Ferland 2003), XSTAR (Kallman 2001) and AtomDB (Foster et al. 2012) used to numerically simulate the thermal and ionization structure of ionized astrophysical nebulae. All of the photoionisation cross sections are available (via email) from the author.

ACKNOWLEDGEMENTS

BMMcL acknowledges support by the US National Science Foundation under the visitors program through a grant to ITAMP at the Harvard-Smithsonian Center for Astrophysics and Queen's University Belfast through a visiting research fellowship (VRF). BMMcL would like to thank Dr. Wayne Stolte and Dr. Alfred Schlachter for their hospitality during numerous visits to the Advanced Light Source in Berkeley, CA, where this work was completed. Professor Phillip Stancil is thanked for a careful reading of this manuscript and for many helpful suggestions. This research used resources of the National Energy Research Scientific Computing Center, which is supported by the Office of Science of the U.S. Department of Energy (DOE) under Contract No. DE-AC02-05CH11231. The computational work was performed at the National Energy Research Scientific Computing Center in Oakland, CA, USA and at The High Performance Computing Center Stuttgart (HLRS) of the University of Stuttgart, Stuttgart, Germany. This research also used resources of the Oak Ridge Leadership Computing Facility at the Oak Ridge National Laboratory, which is supported by the Office of Science of the U.S. Department of Energy (DoE) under Contract No. DE-AC05-00OR22725.

REFERENCES

Angel G. C., Samson J. A. R., 1988, *Phys. Rev. A*, **38**, 5578
 Ballance C. P., 2015, DARC codes website URL, <http://connorb.freeshell.org>

Ballance C. P., Griffin D. C., 2006, *J. Phys. B: At. Mol. Opt. Phys.*, **39**, 3617
 Ballance C. P., McLaughlin B. M., 2015, *J. Phys. B: At. Mol. Opt. Phys.*, **48**, 085201
 Ballance C. P., Berrington K. A., McLaughlin B. M., 1999, *Phys. Rev. A*, **60**, R4217
 Barthel M., Flesch R., Rühl E., McLaughlin B. M., 2015, *Phys. Rev. A*, **91**, 013406
 Berkowitz J., 1979, *Photoabsorption, Photoionization and Photoelectron Spectroscopy*. Academic Press, New York, USA
 Berkowitz J., Batson C. H., Goodman G. L., 1981, *Phys. Rev. A*, **24**, 149
 Berrington K. A., Nakazaki S., 2002, *At. Data Nucl. Data Tables*, **82**, 1
 Burke P. G., 2011, *R-Matrix Theory of Atomic Collisions: Application to Atomic, Molecular and Optical Processes*. Springer, New York, USA
 Burke P. G., Robb W. D., 1975, *Adv. At. Mol. Phys.*, **11**, 143
 Cardelli J. A., Federman S. R., Lambert D. L., Theodosiou C. E., 2000, *Astrophys. J.*, **25**, 513
 Cartlidge E., 2012, *Science*, **336**, 1095
 Cowan R. D., 1981, *The Theory of Atomic Structure and Spectra*. University of California Press, Berkeley, California, USA
 Dupree A. K., 1978, *Adv. At. Mol. Phys.*, **14**, 393
 Dyall K. G., Grant I. P., Johnson C. T., Plummer E. P., 1989, *Comput. Phys. Commun.*, **55**, 425
 Eisberg R. E., Resnik R. M., 1985, *Quantum Physics of Atoms, Molecules, Solids Nuclei and Particles*, 2nd edn. Wiley, New York, USA
 Fano U., Cooper J. W., 1968, *Rev. Mod. Phys.*, **40**, 441
 Feldman P. D., Ake T. B., Berman A. F., Moos H. W., Sahnou D. J., Strobel D. F., Weaver H. A., 2001, *Astrophys. J.*, **554**, L121
 Ferland G. J., 2003, *Ann. Rev. of Astron. Astrophys.*, **41**, 517
 Ferland G. J., Korista K. T., Verner D. A., Ferguson J. W., Kingdon J. B., Verner E. M., 1998, *Pub. Astron. Soc. Pac. (PASP)*, **110**, 761
 Foster A. R., Ji L., Smith R. K., Brickhouse N. S., 2012, *Astrophys. J.*, **756**, 128
 Froese-Fischer C., 1977, *The Hartree – Fock Method for Atoms*. Wiley, New York, USA
 Froese-Fischer C., Brage T., Jonsson P., 1996, *Computational Atomic Structure: An MCHF Approach*. IOP Publishing, Bristol, UK
 Garnett D. R., 1989, *Astrophys. J.*, **345**, 771
 Gibson S. T., Greene J. P., Rušić B., Berkowitz J., 1986, *J. Phys. B: At. Mol. Phys.*, **19**, 2825
 Grant I. P., 2007, *Quantum Theory of Atoms and Molecules: Theory and Computation*. Springer, New York, USA
 Hernández E. M., et al., 2015, *J. Quant. Spec. Rad. Trans.*, **151**, 217
 Hinojosa G., et al., 2012, *Phys. Rev. A*, **86**, 063402
 Kallman T. R., 2001, *Astrophys. J. Suppl. Ser.*, **134**, 139
 Keenan F. P., Ohja P., Hibbert A., 1993, *Phys. Scr.*, **48**, 129
 Keenan F. P., Aller L. H., Exter K. M., Hyung S., Pollacco D. L., 2003, *Astrophys. J.*, **543**, 385
 Kennedy E. T., Mosnier J.-P., Van Kampen P., Cubaynes D., Guilhaud S., Blancard C., McLaughlin B. M., Bizau J.-M., 2014, *Phys. Rev. A*, **90**, 063409
 Kohl J. L., Parkinson W. H., 1973, *Astrophys. J.*, **184**, 641
 Küppers M. E., Schneider N. M., 2000, *Geo. Res. Lett.*, **25**, 513
 Lombardi G. G., Cardon B. L., Kurucz R. L., 1981, *Astrophys. J.*, **248**, 1202
 Macaluso D. A., Aguilar A., Kilcoyne A. L. D., Red E. C., Bilodeau R. C., Phaneuf R. A., C. S. N., McLaughlin B. M., 2015, *Phys. Rev. A*, **92**, 063424
 McLaughlin B. M., Ballance C. P., 2012a, *J. Phys. B: At. Mol. Opt. Phys.*, **45**, 085701

- McLaughlin B. M., Ballance C. P., 2012b, *J. Phys. B: At. Mol. Opt. Phys.*, **45**, 095202
- McLaughlin B. M., Ballance C. P., 2015, in Resch M. M., Kovalenko Y., Fotch E., Bez W., Kobaysah H., eds, , *Sustained Simulated Performance 2014*. Springer, Berlin, Germany, pp 173–190
- McLaughlin B. M., Ballance C. P., Pindzola M. S., Müller A., 2015, in Nagel W. E., Kröner D. H., Resch M. M., eds, , *High Performance Computing in Science and Engineering’14*. Springer, Berlin, Germany, pp 23–40
- McLaughlin B. M., Ballance C. P., Pindzola M. S., Schippers S., Müller A., 2016a, in Nagel W. E., Kröner D. H., Resch M. M., eds, , *High Performance Computing in Science and Engineering’15*. Springer, Berlin, Germany, pp 51–74
- McLaughlin B. M., Ballance C. P., Schippers S., Hellhund J., Kilcoyne A. L. D., Phaneuf R. A., Müller A., 2016b, *J. Phys. B: At. Mol. Opt. Phys.*, **49**, 065201
- Mooney D., Federman S. R., Sheffer Y., 2012, *Astrophys. J.*, **744**, 174
- Müller A., et al., 2014, *J. Phys. B: At. Mol. Opt. Phys.*, **47**, 215202
- Müller A., Schippers S., Hellhund J., Holste K., Kilcoyne A. L. D., Phaneuf R. A., Ballance C. P., McLaughlin B. M., 2015, *J. Phys. B: At. Mol. Opt. Phys.*, **48**, 235203
- Neufeld D. A., Roueff E., Snell R. L., Lis D., Benz O., Bruderer S., 2012, *Astrophys. J.*, **748**, 37
- Norrington P. H., 2004, *J. Phys. B: At. Mol. Opt. Phys.*, **24**, 1803
- Norrington P. H., Grant I. P., 1987, *J. Phys. B: At. Mol. Opt. Phys.*, **20**, 4869
- Ohja P., Hibbert A., 1987, *J. Phys. B: At. Mol. Opt. Phys.*, **22**, 1153
- Opacity Team 1995, *The Opacity Project*. Vol. 1, Institute of Physics Publications, Bristol, UK
- Parpia F., Froese-Fischer C., Grant I. P., 2006, *Comput. Phys. Commun.*, **94**, 249
- Pineau des Forêts G., Roueff E., Flower D. R., 1986, *Mon. Not. Roy. Astron. Soc.*, **223**, 743
- Quigley L., Berrington K. A., 1996, *J. Phys. B: At. Mol. Opt. Phys.*, **29**, 4529
- Quigley L., Berrington K. A., Pelan J., 1998, *Comput. Phys. Commun.*, **114**, 225
- Ralchenko Y., Kramida A. E., Reader, J. and NIST ASD Team 2014, *NIST Atomic Spectra Database (version 5.2)*, National Institute of Standards, Technology, Gaithersburg, MD, USA, <http://physics.nist.gov/>
- Rydberg J. R., 1890, *Phil. Mag.*, **29**, 331
- Rydberg J. R., 1893, *Ann. Phys.*, **50**, 625
- Rydberg J. R., 1894, *Ann. Phys.*, **52**, 119
- Seaton M. J., 1983, *Rep. Prog. Phys.*, **46**, 167
- Sharpee B., Zhang Y., Williams R., Pellegrini E., Cavagnolo K., Badwin J. A., Phillips M., Lui X. W., 2007, *Astrophys. J.*, **659**, 1265
- Shore B. W., 1967, *Rev. Mod. Phys.*, **39**, 439
- Sossah A. M., Tayal S. S., 2012, *Astrophys. J. Suppl. Ser.*, **20**, 12
- Sterling N. C., Dinerstein H. L., Kallman T. R., 2007, *Astrophys. J. Suppl. Ser.*, **169**, 37
- Sylwester B., Phillips K. J. H., Slywester H., Kuznetsov V. D., 2011, *Astrophys. J.*, **738**, 49
- Wijesundera W. P., Parpia F. A., Grant I. P., Norrington P. H., 1991, *J. Phys. B: At. Mol. Opt. Phys.*, **24**, 1803

This paper has been typeset from a \LaTeX file prepared by the author.